All Sciences Proceedings

3rd International Conference on Innovative Academic Studies

September 26-28, 2023 : Konya, Turkey

ICIAS

All Sciences Proceedings
http://as-proceeding.com/

https://www.icias.net/

Micromixing of deionized water and plasma using square-wave microchannels

Narges Jafari Ghahfarrokhi, Mehdi Mosharaf-Dehkordi*

Department of Mechanical Engineering, University of Isfahan, Isfahan, Iran

(m.mosharaf@eng.ui.ac.ir)

Abstract **–** This paper examines the micromixing process in a square-wave-based micromixer to mix deionized water and plasma for biological applications. The numerical simulations are carried out using COMSOL Multiphysics software by utilizing the finite element method (FEM). The performance of three types of square-wave-based micromixer are assessed and it is demonstrated that the micromixer Type III with the most number of cylindrical obstacles in the flow direction has the maximum mixing index. The results reveal that as the inlet velocity is reduced, the values of the mixing index are augmented due to an increment in the residence time of liquids in the micromixer.

Keywords – Microfluidics, Micomixing, Deionized Water, Plasma, Square-Wave Microchannel

I. INTRODUCTION

Micromixers have numerous applications in chemistry and biology [1]. To improve the mixing quality, various active and passive techniques have been utilized by many researchers [2]. Passive methods do not employ external energy sources, while active techniques, such as magnetophoresis [3-4], acoustic force [5-6], electroosmosis [7], etc., utilize external actuators.

Several investigators have utilized serpentine microchannels, curved microchannels, square-wave microchannels, and zigzag microchannels to augment the mixing efficiency of micromixers. For instance, Kuo et al. [8] compared the mixing quality of curved, square-wave, and zigzag microchannels to mix deionized water and plasma and demonstrated that square-wave microchannel results in a higher MI (about 68%) in comparison with the other two cases. Bahrami and Bayareh utilized sinusoidal [9] and twisted microchannels [10] to improve the quality of micromixing. It was found that MI is improved with the wavelength when sinusoidal walls are utilized and is reduced with the twisted angle when twisted walls are employed. They also revealed that the pressure drop is a strong function of the Reynolds number. Babaie et al. [11] considered the impact of Dean flow and separation vortices on the performance of a serpentine micromixer with curved walls and concluded that sinusoidal walls affect the mixing quality significantly. Based on the geometry of revers, Jafari Ghahfarrokhi and Bayareh [12] introduced a novel micromixer to augment MI by creating separation vortices and centrifugal force.

Mondal et al. [13] considered two types of raccoon and serpentine micromixers. It was demonstrated that as the amplitude is enhanced and the wavelength is reduced, the mixing quality is improved. They showed the mixing index of the raccoon type is higher than that of the serpentine micromixer. Nivedita et al. [14] employed a three-dimensional spiral micromixer to enhance the mixing index by creating the Dean vortices in lateral cross-sections. They introduced a critical value for the Dean number to formulate the secondary Dean vortices. It was revealed that the

critical Dean number is reduced with the aspect ratio of the microchannel. Scherr et al. [15] introduced a logarithmic spiral micromixer and found that mixing quality is a decreasing function of the Reynolds number until a Reynolds number of 15. The mixing index then was augmented with the Reynolds number and reached 86% when the Reynolds number was 67. Yang et al. [16] presented a three-dimensional micromixer involving two spiral layers and reached a mixing efficiency of 90% by optimizing the amount of flow rate and micromixer structure. Their assessments were performed numerically and experimentally.

In the present paper, the micromixing of deionized water and plasma is assessed using a square-ware-based microchannel. Besides, the influence of placing some cylindrical obstacles in the channel is examined.

II. Governing Equations

Steady-state governing equations for the micromixing of two incompressible Newtonian fluids are as follows [1]:

Continuity equation:

$$\nabla \cdot \mathbf{u} = 0 \tag{1}$$

Navier-Stokes equation:

$$\rho \frac{\mathrm{D}\mathbf{u}}{\mathrm{D}t} = -\boldsymbol{\nabla} \mathrm{p} + \mu \nabla^2 \mathbf{u} \tag{2}$$

where $\mathbf{u}$ is the velocity, ρ is the density, and p is the pressure.

The convection-diffusion transport equation can be also expressed as:

$$\mathbf{u} \cdot \nabla \mathrm{C} = \mathrm{D} \nabla^2 \mathrm{C} \tag{3}$$

Here, C is the species concentration and *D* is molecular diffusivity.

The mixing index (MI) is calculated as follows:

$$MI = \left(1 - \left(\sqrt{\frac{1}{N} \sum_{i=1}^{N} \left(\frac{c_i - \bar{c}}{\bar{c}} \right)^2} \right) \right) \times 100 \tag{4}$$

where N denotes the number of nodes in the considered area.

III. Results

In this section, firstly, the micromixing process is evaluated by considering a square-wave-based micromixer (Fig. 1) to mix deionized water and plasma. Table 1 presents their properties. There are three types of micromixers in the present work. Type I has no cylindrical obstacles in the flow direction and Types II and III have various numbers of obstacles.

The grid independence test is performed to ensure that the numerical results do not depend on the number of grid points. Figs. 2a, 2b, and 2c illustrate the variations of concentration in a longitudinal section, velocity in a longitudinal section, and velocity distribution at a lateral cross-section, respectively. It should be pointed out that the examination of the velocity profile is necessary to avoid artificial errors [17]. These figures demonstrate that the extra fine grid can be selected for the present simulations.

Table 1. Properties of deionized water and plasma [8].

	Deionized water	Plasma
Diffusivity, m^2/s	1.2×10^{-9}	2.1×10^{-10}
Density, $kg/^{m3}$	997	1025
Viscosity, kg/m.s	0.9×10^{-3}	1.5×10^{-3}

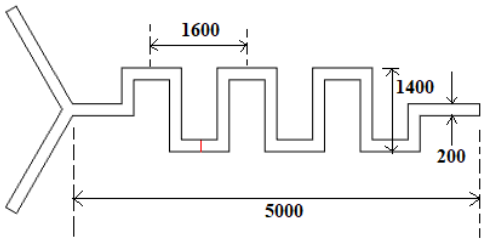

Fig. 1. Schematic of the square-wave-based micromixer. The dimensions are in micrometers.

Fig. 3 depicts the concentration contours for the above-mentioned micromixers, indicating that the micromixer Type III can provide better mixing quality. This is confirmed by calculating the amount of MI quantitatively which is demonstrated in Fig. 4. This figure shows that the value of MI at the outlet of micromixers Type I, Type II, and Type III is 88.8%, 91.22%, and 93.27%, respectively. The presence of cylindrical obstacles has a positive effect on the enhancement of MI. Even though, due to the low velocity of two liquids, a vortex is not created at the rear of obstacles, the stretching and folding lead to better mixing of two liquids. In other words, the obstacles narrow the flow direction and then expand it, resulting in the creation of stretching and folding phenomenon.

It is known that inlet velocity has a great impact on the micromixing process [1]. The influence of inlet velocity is now considered for the Type III of the above-mentioned micromixers. Fig. 5 demonstrates

that the mixing quality is improved when the Reynolds number, i.e. inlet velocity, is reduced. This is because the residence time is augmented when the liquid velocity is reduced. Hence, two liquids have more time for mixing due to the diffusions at their interfaces. It should be noted that the dominant mechanism of micromixing is molecular diffusion when the amount of Reynolds number is low. Even though the values of MI are too high quantitatively (Fig. 6), it is expected that the amounts of the pressure drop to be high similarly. Thus, an optimal case should be determined.

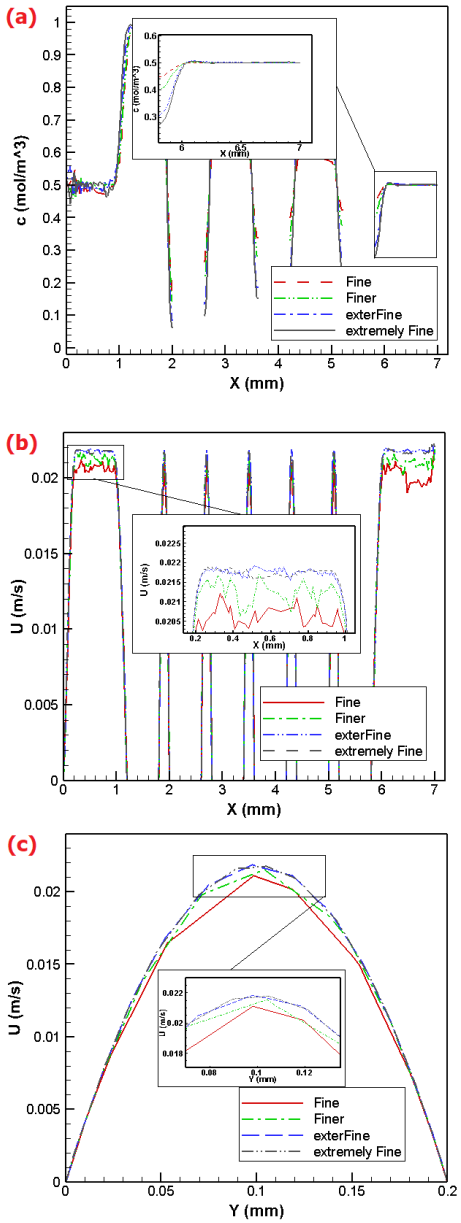

Fig. 2. (a) Variations of concentration in a longitudinal section, (b) variations of velocity in a longitudinal section, and (c) velocity distribution at a lateral cross-section.

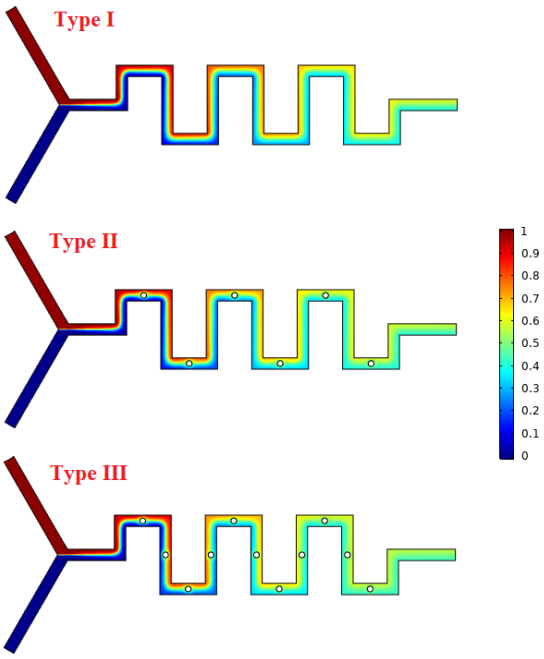

Fig. 3. Concentration contours for three types of micromixers.

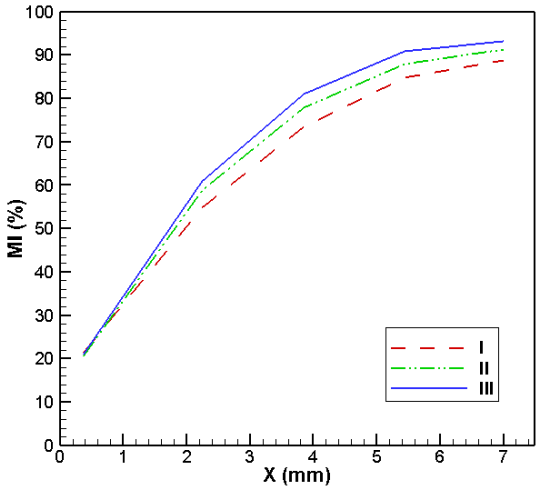

Fig. 4. Variations of MI along the micromixer for three types of micromixers.

IV. Conclusion

The present paper considered a biological application of microfluidic devices in micromixers. This numerical study assesses the micromixing of deionized water and plasma in square-wave-based micromixers utilizing the FEM. It is concluded that the micromixer Type III, in which 11 cylindrical obstacles are used in the flow direction, has the maximum mixing index. The results demonstrate that as the inlet velocity is reduced, the values of the mixing index are enhanced due to an increment in the liquid's residence time in the micromixer.

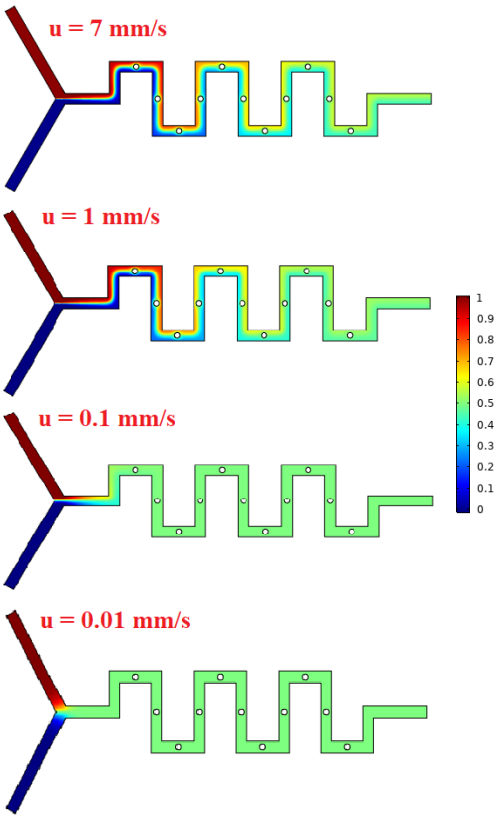

Fig. 5. Concentration contours for the micromixer Type III at various inlet velocities.

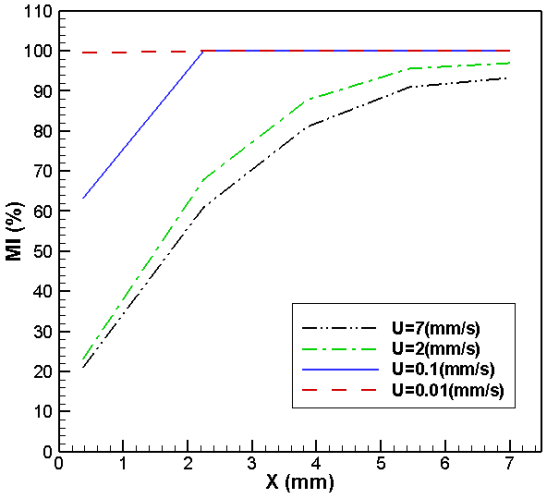

Fig. 6. Variations of MI along the micromixer Type III for various inlet velocities.

REFERENCES

[1] M. Bayareh, M. Nazemi Ashani, A. Usefian, "Active and passive micromixers: A comprehensive review," *Chemical Engineering and Processing-Process Intensification*, vol. 147, p. 107771, 2020.

[2] Z. Ghorbani Kharaji, M. Bayareh, V. Kalantar, "A review on acoustic field-driven micromixers," *Int. J. Chem. React. Eng*. vol. 19, pp. 553-569, 2021.

[3] D. Bahrami, A. Ahmadi Nadooshan, M. Bayareh, "Numerical Study on the Effect of Planar Normal and Halbach Magnet Arrays on Micromixing," *Int. J. Chem. React. Eng*. vol. 18, pp. 20200080, 2020.

[4] D. Bahrami, A. Ahmadi Nadooshan, M. Bayareh, "Effect of non-uniform magnetic field on mixing index of a sinusoidal micromixer," *Korean J. Chem. Eng*. vol. 39, pp. 316–327, 2021.

[5] Z. Ghorbani Kharaji, V. Kalantar, M. Bayareh, "Acoustic sharp-edge-based micromixer: a numerical study," *Chem. Pap*. vol. 76, pp. 1721–1738, 2021.

[6] Z. Ghorbani Kharaji, V. Kalantar, M. Bayareh, "Mixing enhancement in an acousto-inertial microfluidic system," *Chemical Engineering and Processing-Process Intensification*, vol. 191, p. 109473, 2023.

[7] N. Jafari Ghahfarokhi, M. Bayareh, A. Ahmadi Nadooshan, S. Azadi, "Mixing enhancement in electroosmotic micromixers," *Journal of Thermal Engineering*, vol. 7(2), pp. 47-57, 2020.

[8] J.-N. Kuo, H.-S. Liao, X.-M. Li, "Design optimization of capillary-driven micromixer with square-wave microchannel for blood plasma mixing," *Microsystem Technologies*, vol. 23(3), pp. 721–730, 2015.

[9] D. Bahrami, M. Bayareh, "Experimental and numerical investigation of a novel micromixer with sinusoidal channel walls," *Chemical Engineering Technology*, vol. 45(1), pp. 100-109, 2022.

[10] D. Bahrami, M. Bayareh, "Impacts of channel wall twisting on the mixing enhancement of a novel spiral micromixer," *Chem. Pap.*, vol. 76, pp. 465–476, 2022.

[11] Z. Babaie, D. Bahrami, M. Bayareh, "Investigation of a novel serpentine micromixer based on Dean flow and separation vortices," *Meccanica*, vol. 57, pp. 73–86, 2022.

[12] N. Jafari Ghahfarokhi, M. Bayareh, "Numerical study of a novel spiral-type micromixer for low Reynolds number regime," *Korea-Australia Rheology Journal*, vol. 33, pp. 333–342, 2021.

[13] B. Mondal, S.K. Mehta, P.K. Patowari, S. Pati, "Numerical study of mixing in wavy micromixers: comparison between raccoon and serpentine mixer," *Chemical Engineering and Processing - Process Intensification*, vol. 136, pp. 44-61, 2018.

[14] N. Nivedita, P. Ligrani, I. Papautsky, "Dean Flow Dynamics in Low-Aspect Ratio Spiral Microchannels," *Scientific Reports*, vol. 7(1), pp. 1-10, 2017.

[15] T. Scherr, C. Quitadamo, P. Tesvich, D. S.-W. Park, T. Tiersch, D. Hayes, W.T. Monroe, "A planar microfluidic mixer based on logarithmic spirals," Journal of Micromechanics and Microengineering, vol. 22(5), p. 055019, 2012.

[16] J. Yang, L. Qi, Y. Chen, H. Ma, "Design and Fabrication of a Three Dimensional Spiral Micromixer," *Chinese Journal of Chemistry*, vol. 31(2), pp. 209–214, 2012.

[17] M. Bayareh, "Artificial Diffusion in the Simulation of Micromixers: A Review," *Proc. Inst. Mech. Eng., Part C*. vol. 253, pp. 5288-5296, 2020